Pipette aspiration testing of soft tissues

Argatov, Ivan; Mishuris, Gennady

Published in:
Proceedings of the Royal Society A: Mathematical, Physical and Engineering Sciences

DOI:
10.1098/rspa.2016.0559

Publication date:
2016

Citation for published version (APA):
Argatov, I., & Mishuris, G. (2016). Pipette aspiration testing of soft tissues: the elastic half-space model revisited. *Proceedings of the Royal Society A: Mathematical, Physical and Engineering Sciences*, *472*(2193), Article 20160559. https://doi.org/10.1098/rspa.2016.0559

Pipette aspiration testing of soft tissues: The elastic half-space model revisited

Ivan Argatov[1] and Gennady Mishuris[2*]

[1] *Institut für Mechanik, Technische Universität Berlin, Straße des 17. Juni 135, 10623 Berlin, Germany*
[2] *Department of Mathematics, Aberystwyth University, Ceredigion SY23 3BZ, Wales, UK*

Subject Mechanics, mechanical engineering, applied mathematics
Keywords: Pipette aspiration, elastic half-space, transversely isotropic, asymptotic solution

Abstract

The pipette aspiration testing technique is considered, and the elastic half-space model, which was originally introduced in the isotropic incompressible case, is revisited and generalized for the case of transverse isotropy. Asymptotic solutions are obtained in the two limiting cases of a wide and a narrow pipette.

1 Introduction

In recent years, the micropipette aspiration technique was widely used for testing living cells and measuring their mechanical properties [2, 1, 3, 4]. In particular, the cell response is quantified in terms of the aspiration length, which measures projection of the cell into the micropipette under the applied negative pressure.

Being originally developed to handle cells under the microscope and later to investigate their mechanical properties, the pipette aspiration technique is nowadays successfully applied for non-invasive measuring the *in vivo* mechanical behavior of soft human tissues [5, 6]. Also, the pipette aspiration method was used for the local stiffness measurement of soft materials [7, 8].

Recently, the pipette aspiration technique was applied to characterization of nonhomogeneous (fiber reinforced), transversely isotropic materials [9]. Comparison of the pipette aspiration testing method with other mechanical testing techniques utilized for biomaterials (including macroscale testing and nanoindentation) was performed very recently in [10].

The effective application of the pipette aspiration testing technique requires relation between the aspirated length and the applied pressure difference. Theret et al. [11] developed the so-called half-space model under the assumptions that the tested specimen is idealized to be an incompressible, homogeneous, and isotropic elastic medium undergoing small strains.

In their work, the following analytical relationship between the applied pressure difference, ΔP, and the resulting aspirated length, L, has been established:

$$\frac{L}{b} = \frac{3\Delta P}{2\pi E}\Phi(\eta). \tag{1}$$

Here, b is the inner pipette radius, E is the Young's elastic modulus, $\Phi(\eta)$ is a dimensionless factor, called the pipette wall function, and η is the ratio of the pipette thickness to the inner pipette radius.

*corresponding author: ggm@aber.ac.uk

Theret et al. [11] provided two analytical approaches to evaluate the pipette wall function. The first method requires solving an integral equation of the punch problem, while the second approach is based on the local force balance and approximately satisfies the non-penetration contact condition. The corresponding solutions are denoted by $\Phi_P(\eta)$ and $\Phi_F(\eta)$, respectively. The advantage of the force approximate model is that the corresponding wall function is given in an explicit form as

$$\Phi_F(\eta) = \frac{1+\eta}{1+\eta/2}\left\{\frac{\pi}{2} - 1 + \frac{1}{\eta}\left(\mathbf{E}\Big(\frac{1}{1+\eta}\Big) - 1\right)\right\}, \tag{2}$$

where $\mathbf{E}(k)$ is the complete elliptic integral of the second kind. From Fig. 1 it may be seen that the two approaches yield fairly close values of $\Phi(\eta)$ for values of η near 0.2.

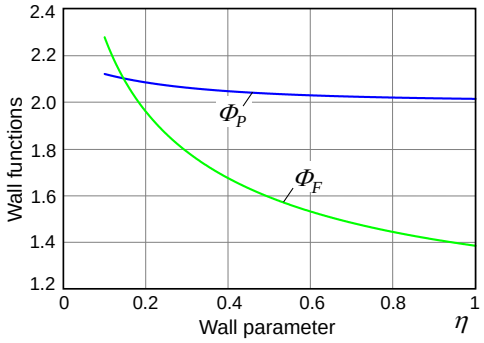

Figure 1: The force model wall function $\Phi_F(\eta)$ and the punch model wall function $\Phi_P(\eta)$ for values of the wall parameter η ranging from 0.1 and 1.0 (after Theret et al. [11])

Further development of the theory was associated with application of numerical methods to evaluate the pipette wall function for a layered elastic medium [7]. It was also shown by Aoki et al. [7] that the friction between the pipette and the specimen surface does not play any significant role. Later, a boundary integral equation model was developed by Haider and Guilak [2] to account for the spherical geometry under the same constitutive assumptions as in the half-space model [11]. The influence of sample thickness in the micropipette aspiration was studied by Alexopoulos et al. [12], Sakamoto and Kobayashi [13], and Boudou et al. [14].

The half-space model [11] has been most widely adopted for extracting the stiffness characteristics via the pipette aspiration [3, 14, 10, 15], which is however applicable provided the tested specimen can be regarded as a relatively large piece of elastic continuum compared with the inner pipette diameter.

However, there is still uncertainty about the significant difference between $\Phi_P(\eta)$ and $\Phi_F(\eta)$ in a wide range of values of η. The present paper addresses this issue, and, moreover, in the limit cases of wide or narrow pipettes, asymptotic solutions for $\Phi_P(\eta)$ are presented, which are accurate enough to deal with a complete range of the wall parameter η.

Furthermore, it represents a practical interest to extend the half-space model for the case of a transversely isotropic material. Under the assumption of frictionless contact between the pipette and the surface of specimen, this extension is made via the reduction of the pipette punch problem to the corresponding contact problem. In this case, formula (1) can be generalized as follows:

$$\frac{L}{b} = \frac{2\Delta P}{\pi M_3}\Phi(\eta). \tag{3}$$

Here, M_3 is the so-called the indentation elastic modulus [16]. In the case of transversely isotropic material, it can be expressed in terms of the material stiffnesses in the following form [17]:

$$M_3 = \frac{2\sqrt{A_{44}}(A_{11}A_{33} - A_{13}^2)}{\sqrt{A_{11}}\big(\sqrt{A_{11}A_{33}} - A_{13}\big)^{1/2}\big(A_{13} + 2A_{44} + \sqrt{A_{11}A_{33}}\big)^{1/2}}. \tag{4}$$

Here, A_{11}, A_{13}, A_{33}, and A_{44} are four independent elastic constants, which are related to the engineering elastic constants (E, E', ν, ν', and G') by the formulas $A_{44} = G'$ and

$$A_{11} = \frac{E\Big(1 - \dfrac{E}{E'}\,\nu'^2\Big)}{(1+\nu)\Big(1 - \nu - \dfrac{2E}{E'}\,\nu'^2\Big)}, \quad A_{13} = \frac{E\nu'}{1 - \nu - \dfrac{2E}{E'}\,\nu'^2}, \quad A_{33} = \frac{E'(1-\nu)}{1 - \nu - \dfrac{2E}{E'}\,\nu'^2}.$$

In the isotropic case, we have

$$M_3 = \frac{E}{1-\nu^2}, \tag{5}$$

where ν is the Poisson's ratio. Note that for an incompressible isotropic materials, when $\nu = 1/2$, in light of (5), formula (3) reduces to (1).

The rest of the paper is organized as follows. In Section 2, the pipette aspiration problem for a transversely isotropic half-space specimen is formulated and asymptotic conditions at infinity are imposed, which distinguish two different cases of a fixed specimen (see Section 22.1) and a free-standing specimen (see Section 22.2). In Section 3, the pipette aspiration problem is reduced to a contact problem for an annular indenter with a non-flat base. We note here that different aspects of the contact problem for an annular indenter were studied in a large number of papers (see, e.g., [18, 19, 20, 21, 22, 23]), and recently it has attracted considerable attention in the case of adhesive contact [24, 25, 26]. The indentation problem for an annular indenter is solved by asymptotic methods in Section 4. In Section 5, an asymptotic solution of the pipette punch problem is obtained in the case of a thick pipette. The case of a narrow pipette is treated by another asymptotic method in Section 6. Finally, in Section 7, the discussion of obtained results is outlined.

2 Pipette aspiration problem formulation

Let us assume that a cylindrical flat-ended pipette with inner radius b and outer pipette radius a is used to aspirate a circular portion, $0 \le r < b$, of the surface of a transversely isotropic elastic half-space $z > 0$, where (r, z) are cylindrical coordinates (see Fig. 2).

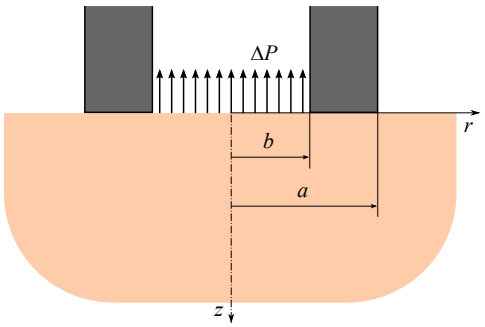

Figure 2: Schematic representation of the elastic half-space model for the pipette aspiration

The wall parameter, which is defined as the ratio of the wall thickness, $2h = a - b$, to the inside radius b, i.e.,

$$\eta = \frac{a-b}{b}, \tag{6}$$

takes values between 0 (very narrow pipette) and infinity (very thick pipette).

It is assumed that the stress imposed by the pipette on the half-space surface (due to the pressure difference ΔP) is constant over the inner circular region, while the outside region is stress-free, that is

$$\sigma_z\big|_{z=0} = \Delta P, \quad 0 \le r < b; \qquad \sigma_z\big|_{z=0} = 0, \quad r > a. \tag{7}$$

Further, the shear stress is assumed to vanish on the entire surface of the elastic half-space, while within the annular contact region, $b \le r \le a$, the normal displacement of the half-space surface is equal to zero (any deformation of the pipette is neglected), i.e.,

$$\sigma_{rz}\big|_{z=0} = 0, \quad 0 \le r < \infty; \qquad u_z\big|_{z=0} = 0, \quad b \le r \le a. \tag{8}$$

It is of practical interest, to measure the aspiration length

$$L = -u_z\big|_{z=0,\ r=0} \tag{9}$$

inside the pipette at its center as a function of the applied pressure difference ΔP.

Now, we distinguish two different ways of fixing the tested specimen (see Fig. 3).

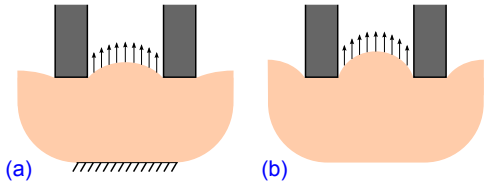

Figure 3: Schematic representation of the pipette aspiration of a relatively large specimen: a) the tested specimen is fixed; b) the tested specimen is free to move due to aspiration

2.1 Pipette aspiration of a fixed specimen

If the half-space specimen is assumed to be fixed at infinity (see Fig. 3a), we impose the following asymptotic condition for the displacement vector:

$$\mathbf{u}(r,z) = o(1), \quad \sqrt{r^2+z^2} \to \infty. \tag{10}$$

In other words the displacements should vanish at infinity.

2.2 Pipette aspiration of a free-standing specimen

If the half-space specimen is allowed to freely move upward due to aspiration (see Fig. 3b), we impose the following asymptotic condition:

$$\mathbf{u}(r,z) = \delta_0 \mathbf{e}_z + o(1), \quad \sqrt{r^2+z^2} \to \infty. \tag{11}$$

Here, $\mathbf{e}_z$ is the unit vector in the downward direction, δ_0 is an unknown vertical displacement of the specimen. The constant δ_0 should be determined from the equilibrium equation

$$\pi b^2 \Delta P = 2\pi \int_b^a p(\rho)\rho \, d\rho, \tag{12}$$

where $p(r)$ is the contact pressure distribution under the pipette, i.e.,

$$p(r) = -\sigma_z\big|_{z=0}, \quad b < r < a.$$

Note that in light of (12), the following asymptotic condition at infinity should hold:

$$\sigma_z(r,z) = O((r^2+z^2)^{-3/2}), \quad \sqrt{r^2+z^2} \to \infty.$$

At the same time, in the case of a fixed specimen (see Section 22.1), it can be shown (see, e.g., [27]) that $\sigma_z(r,z) = O((r^2+z^2)^{-1})$, when $\sqrt{r^2+z^2} \to \infty$.

3 Reduction of pipette aspiration problem to a contact problem

In the absence of the pipette, according to the known solution of Love's circular patch problem [28, 29, 30], the vertical surface displacement profile of the elastic half-space loaded by negative uniform pressure, $-\Delta P$, acting over a circular region of radius b is given by

$$u_z^0(r) = -\frac{4\Delta P}{\pi M_3}\begin{cases} b\mathbf{E}\Big(\dfrac{r}{b}\Big), & 0 \le r \le b, \\ r\Big\{\mathbf{E}\Big(\dfrac{b}{r}\Big) - \Big(1 - \dfrac{b^2}{r^2}\Big)\mathbf{K}\Big(\dfrac{b}{r}\Big)\Big\}, & r \ge b, \end{cases} \tag{13}$$

where M_3 is the indentation modulus of the elastic half-space (see Eq. (4)), $\mathbf{K}(k)$ and $\mathbf{E}(k)$ are, respectively, the complete elliptic integrals of the first and second kind of the modulus $k \in [0, 1)$.

Therefore, the contact pressure, $p(r)$, under the pipette punch should satisfy the following integral equation:

$$\frac{1}{\pi M_3}\int_0^{2\pi} d\phi \int_b^a \frac{p(\rho)\rho\, d\rho}{\sqrt{r^2 + \rho^2 - 2r\rho\cos\phi}} = -u_z^0(r) - \delta_0, \tag{14}$$

where $u_z^0(r)$ is given by the second formula (13), while δ_0 is equal to zero for a fixed tested specimen (Fig. 3a), or should be determined from the equilibrium equation (12) in the case of a free standing specimen (Fig. 3b).

According to the principle of superposition, the aspirated length is evaluated as the sum

$$L_0 = -u_z^0(0) - \delta_0 - \frac{2}{M_3}\int_b^a p(\rho)\, d\rho, \tag{15}$$

where, in light of the first formula (13), we have

$$-u_z^0(0) = \frac{2b\Delta P}{M_3}. \tag{16}$$

In the case of a fixed specimen, when $\delta_0 = 0$, formula (16) reduces to

$$L = -u_z^0(0) - \frac{2}{M_3}\int_b^a p(\rho)\, d\rho. \tag{17}$$

Therefore, in view of (14) and (16), formulas (15) and (17) can be represented in the following form (which generalizes Eq. (1) introduced in [11]):

$$L_0 = \frac{2b\Delta P}{\pi M_3}\Phi_P^0(\eta), \tag{18}$$

$$L = \frac{2b\Delta P}{\pi M_3}\Phi_P(\eta). \tag{19}$$

Here, $\Phi_P^0(\eta)$ are $\Phi_P(\eta)$ are the so-called pipette wall functions (for a free-standing and a fixed specimen, respectively); they depend solely on the wall parameter η, which was introduced by (6). Thus, the pipette aspiration problem (7), (8) is reduced to solving the integral equation (14) of contact problem for a frictionless annular punch.

4 Indentation of an elastic half-space by an annular punch

4.1 Governing integral equation of the contact problem and the surface deflection for a flat-ended annular punch

We consider the frictionless indentation of an elastic half-space $z > 0$ by a rigid axisymmetric punch with a ring-shaped contact region $b < r < a$. This problem was studied in detail in a number of papers [18, 19, 21, 22]. In particular, the contact pressure $p(r)$ under a flat-ended punch satisfies the integral equation

$$\frac{1}{\pi M_3}\int\limits_0^{2\pi} d\phi \int\limits_b^a \frac{p(\rho)\rho\, d\rho}{\sqrt{r^2+\rho^2-2r\rho\cos\phi}} = \delta_0, \quad b < r < a, \tag{20}$$

where M_3 is the indentation elastic modulus, a and b are the outer and the inner radii of the contact area, δ_0 is the punch displacement.

In the equilibrium state, the contact force is given by

$$F = 2\pi \int\limits_b^a p(\rho)\rho\, d\rho, \tag{21}$$

Following Gubenko and Mossakovskii [18] and applying the method developoed by Collins [31], the solution of Eq. (20) is reduced to the Fredholm integral equation of the second kind

$$y(x) + \frac{2}{\pi^2}\int\limits_0^1 \frac{y(\xi)}{x^2+\xi^2}\left[\xi\ln\left(\frac{1-\lambda x}{1+\lambda x}\right) - x\ln\left(\frac{1-\lambda\xi}{1+\lambda\xi}\right)\right]d\xi = -\frac{1}{2\lambda}\ln\left(\frac{1-\lambda x}{1+\lambda x}\right). \tag{22}$$

Accordingly, the contact pressure is given by

$$\frac{2a}{M_3\delta_0}p(r) = \frac{2}{\pi}\frac{1}{\sqrt{1-\lambda^2\rho^2}} - \frac{8}{\pi^3}\frac{1}{\rho}\frac{d}{d\rho}\int\limits_0^1 \frac{xy(x)}{\sqrt{\rho^2-x^2}}\,\mathrm{atan}\sqrt{\frac{1-\lambda^2\rho^2}{\rho^2-x^2}}\,dx, \tag{23}$$

where $\rho = r/b$, so that $\rho > 1$ under the punch.

At the same time, the surface deflection inside the flat-ended annular punch is evaluated as

$$\frac{u_3(r)}{\delta_0} = 1 - \frac{4\lambda}{\pi^2}\int\limits_{r/b}^1 \left(x^2 - \frac{r^2}{b^2}\right)^{-1/2} y(x)\,dx \qquad (0 \le r \le b),$$

so that the surface deflection at the origin of coordinates is

$$\frac{u_3(0)}{\delta_0} = 1 - \frac{4\lambda}{\pi^2}\int\limits_0^1 \frac{y(x)}{x}\,dx \tag{24}$$

Note finally [31] that while Eq. (22) holds for all values of a and b, approximate solutions can be only readily be obtained when $b \ll a$ (i.e., for a wide punch).

4.2 Indentation by a wide flat-ended annular punch

Let the contact radii ratio

$$\lambda = \frac{b}{a} \tag{25}$$

be small. Then, the iterative solution of Eq. (22) can be obtained in the form

$$\begin{aligned} y(x)=&x + \lambda^2\frac{x^3}{3} + \lambda^3\frac{4x}{9\pi^2} + \lambda^4\frac{x^5}{5} + \lambda^5\frac{4x}{225\pi^2}(15x^2+14) \\ &+ \lambda^6\left(\frac{x^7}{7} + \frac{16x}{81\pi^4}\right) + \lambda^7\frac{4x}{3675\pi^2}(175x^4+154x^2+145) \\ &+ \lambda^8\left(\frac{x^9}{9} + \frac{16x(15x^2+32)}{2025\pi^4}\right) + O(\lambda^9). \end{aligned} \tag{26}$$

The terms to $O(\lambda^6)$ agree with those given by Collins [31].

Now, by making use of Eqs. (21), (23) and the asymptotic expansion (26), the following approximation for the contact force can be established [31, 32]:

$$F = 2M_3 a\delta_0\left\{1 - \frac{4\lambda^3}{3\pi^2} - \frac{8\lambda^5}{15\pi^2} - \frac{16\lambda^6}{27\pi^4} - \frac{92\lambda^7}{315\pi^2} - \frac{448\lambda^8}{675\pi^4} + O(\lambda^9)\right\}. \tag{27}$$

Finally, according to (24) and (26), the surface deflection at the origin of coordinates can be evaluated as

$$\begin{aligned} \frac{u_3(0)}{\delta_0}=&1 - \frac{4\lambda}{\pi^2} - \frac{4\lambda^3}{9\pi^2} - \frac{16\lambda^4}{9\pi^4} - \frac{4\lambda^5}{25\pi^2} - \lambda^6\frac{304}{225\pi^4} \\ &- \frac{4\lambda^7}{\pi^6}\left(\frac{16}{81} + \frac{\pi^4}{49}\right) - \lambda^8\frac{11104}{11025\pi^4} + O(\lambda^9). \end{aligned} \tag{28}$$

We can observe evidently that $u_3(0) \to \delta_0$ as $\lambda \to 0$.

4.3 Indentation by a narrow flat-ended annular punch

Let us introduce the notation

$$R = \frac{1}{2}(a+b), \quad h = \frac{1}{2}(a-b), \quad \varepsilon = \frac{h}{R}. \tag{29}$$

Now, we assume that the parameter $\varepsilon = (1-\lambda)(1+\lambda)$, where λ is the contact radii ratio (25), is small, and thus, λ is close to 1.

In this case, the solution of Eq. (20) can be represented in the form

$$p(r) = \frac{\pi M_3 v(\varepsilon,\alpha)}{\varepsilon R(1+\varepsilon\cos\alpha)\sin\alpha}, \quad \alpha = \arccos\frac{(r-R)}{h}, \tag{30}$$

so that the contact force is evaluated as follows:

$$F = 2\pi^2 M_3 R\int\limits_0^\pi v(\varepsilon,\alpha)\,d\alpha. \tag{31}$$

Now, applying the asymptotic method developed by Grinberg and Kuritsyn [33] (see also [20]), we obtain

$$\begin{aligned} v(\varepsilon,\alpha)=&\frac{\delta_0}{2\pi\Lambda} + \frac{\varepsilon\delta_0}{4\pi}\cos\alpha \\ &+ \frac{\varepsilon^2\delta_0}{32\pi}\left[2 - \frac{5}{\Lambda} + \frac{4}{\Lambda^2} + \left(1 - \frac{3}{2\Lambda}\right)\cos 2\alpha\right] \\ &+ \frac{\varepsilon^3\delta_0}{256\pi}\left\{\left(9 - \frac{6}{\Lambda} - 4\Lambda\right)\cos\alpha - \left(3 - \frac{6}{\Lambda}\right)\cos 3\alpha\right\} + \dots . \end{aligned} \tag{32}$$

Further, from (31) and (32) it follows that

$$F = \pi^2 M_3 R \delta_0 \left\{ \frac{1}{\Lambda} + \frac{\varepsilon^2}{16} \left(2 - \frac{5}{\Lambda} + \frac{4}{\Lambda^2} \right) + \dots \right\}. \tag{33}$$

Finally, the surface deflection at the origin of coordinates can be evaluated as

$$\frac{u_3(0)}{\pi \delta_0} = \frac{1}{\Lambda} + \frac{\varepsilon^2}{16\Lambda^2} \left(2\Lambda^2 - 5\Lambda + 4 \right) + \dots, \tag{34}$$

where we have introduced the notation

$$\Lambda = \ln \frac{16}{\varepsilon}. \tag{35}$$

Note that Λ becomes a large parameter when $\varepsilon \to 0$.

4.4 Harmonic capacity and the center deflection for an annular punch

For a flat-ended punch, the force-displacement relation can be represented in the form

$$F = \pi M_3 \mathbf{c} \delta_0, \tag{36}$$

where $\mathbf{c}$ is the harmonic capacity of the contact area (see, in particular, [34, 35, 36]).

In the case of an annular contact area with the inner, b, and the outer, a, radii, according to Eqs. (27), (33), and (36), the following asymptotic approximations hold:

$$\mathbf{c} = \frac{2a}{\pi} \left\{ 1 - \frac{4\lambda^3}{3\pi^2} - \frac{8\lambda^5}{15\pi^2} - \frac{16\lambda^6}{27\pi^4} - \frac{92\lambda^7}{315\pi^2} - \frac{448\lambda^8}{675\pi^4} + \dots \right\} \tag{37}$$

for $\lambda \ll 1$, and

$$\mathbf{c} = \pi R \left\{ \frac{1}{\Lambda} + \frac{\varepsilon^2}{16} \left(2 - \frac{5}{\Lambda} + \frac{4}{\Lambda^2} \right) + \dots \right\}, \tag{38}$$

for $\varepsilon \ll 1$. Here, R and Λ are given by (29) and (35).

It is interesting to observe that the simple asymptotic formula (38), although being derived for small ε only, works well in the whole range of the parameter $\varepsilon \in (0, 1)$ (see Fig. 4). Indeed, the difference between the predictions of the asymptotic formulas (37) and (38) is less than 0.05% in the range of small λ.

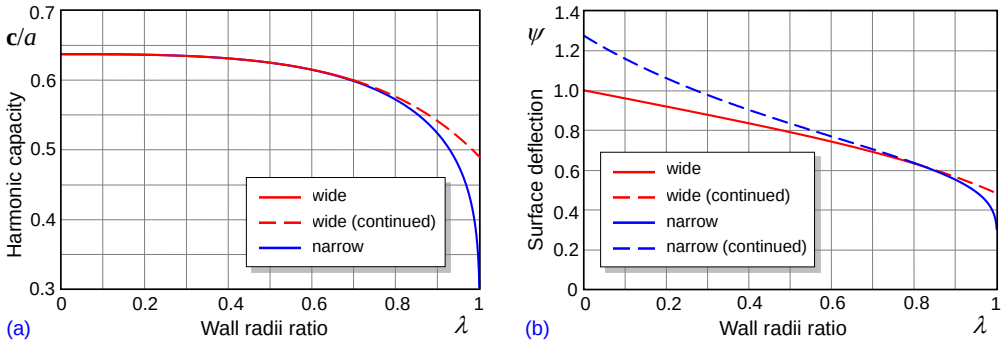

Figure 4: The harmonic capacity and the center deflection for an annular flat-ended punch: (a) The red and blue lines are drawn according to the asymptotic approximations (37) and (38), respectively; (b) The red and blue lines are drawn according to the asymptotic approximations (40) and (41), respectively

Further, the vertical (normal) displacement of the surface of an elastic half-space at the center of a flat-ended annular punch can be represented in the form

$$u_3(0) = \psi \delta_0, \tag{39}$$

where ψ is a dimensionless factor.

According to Eq. (39) and the asymptotic expansions (28) and (34), the following approximations hold:

$$\psi{=}1-\frac{4\lambda}{\pi^2}-\frac{4\lambda^3}{9\pi^2}-\frac{16\lambda^4}{9\pi^4}-\frac{4\lambda^5}{25\pi^2}-\lambda^6\frac{304}{225\pi^4}\\ -\frac{4\lambda^7}{\pi^6}\Big(\frac{16}{81}+\frac{\pi^4}{49}\Big)-\lambda^8\frac{11104}{11025\pi^4}+\ldots, \tag{40}$$

for $\lambda \ll 1$, and

$$\psi=\frac{\pi}{\Lambda}+\frac{\varepsilon^2\pi}{16\Lambda^2}\big(2\Lambda^2-5\Lambda+4\big)+\ldots, \tag{41}$$

for $\varepsilon \ll 1$.

Formulas (37), (40) and (38), (41) should be used in the cases of wide and narrow annular punches, respectively. Fig. 4 shows that the obtained asymptotic solutions cover the whole range of the parameter $\lambda \in (0,1)$.

5 Solution of the pipette punch problem for a thick pipette

5.1 Governing integral equation in the case of a fixed half-space specimen

Following Theret et al. [11], the pipette punch problem (14) with $\delta_0 = 0$ can be reduced to the problem of determining a certain function $\chi(r,z)$, harmonic in the half-space $z > 0$, vanishing at infinity and satisfying the boundary conditions

$$\frac{\partial\chi}{\partial z}(r,0)=1, \quad r\in(0,b), \quad \chi(r,0)=0, \quad r\in(b,a), \quad \frac{\partial\chi}{\partial z}(r,0)=0, \quad a<r.$$

According to the method developed in [31, 18], this harmonic potential appears as follows [11]:

$$\chi(r,z){=}\frac{1}{2\mathrm{i}}\int\limits_0^b g(t)\bigg[\frac{1}{(r^2+(z-\mathrm{i}t)^2)^{1/2}}-\frac{1}{(r^2+(z+\mathrm{i}t)^2)^{1/2}}\bigg]dt\\ +\frac{1}{2}\int\limits_a^\infty j(t)\bigg[\frac{1}{(r^2+(z-\mathrm{i}t)^2)^{1/2}}+\frac{1}{(r^2+(z+\mathrm{i}t)^2)^{1/2}}\bigg]dt.$$

Here, $j(t)$ is a real-valued function given by

$$j(t)=\frac{2}{\pi}\int\limits_0^b\frac{sg(s)}{t^2-s^2}\,ds, \tag{42}$$

while $g(t)$ is a real *odd* function, which satisfies the linear integral equation

$$g(t)+\frac{2}{\pi^2}\int\limits_0^b\frac{g(s)}{t^2-s^2}\bigg[s\ln\Big(\frac{a-t}{a+t}\Big)-t\ln\Big(\frac{a-s}{a+s}\Big)\bigg]ds=-\frac{2t}{\pi}, \tag{43}$$

where $0 \le t \le b$.

At the same time, the surface profile is given by

$$\begin{aligned} u_z(r,0) &= -\frac{2\Delta P}{M_3}\int_r^b \frac{g(t)\,dt}{\sqrt{t^2-r^2}} \quad \text{for} \quad 0 \le r < b, \\ &= 0 \quad \text{for} \quad b \le r \le a, \\ &= \frac{2\Delta P}{M_3}\int_a^r \frac{j(t)\,dt}{\sqrt{r^2-t^2}} \quad \text{for} \quad r > a, \end{aligned} \tag{44}$$

and the contact pressure under the pipette punch is given by

$$p(r) = \frac{\Delta P}{r}\frac{d}{dr}\left(\int_0^b \frac{tg(t)\,dt}{\sqrt{r^2-t^2}} - \int_a^\infty \frac{tj(t)\,dt}{\sqrt{t^2-r^2}}\right), \tag{45}$$

where $r \in (b, a)$.

According to (44), the aspiration length is calculated as follows:

$$L = -u_z(0,0) = \frac{2\Delta P}{M_3}\int_0^b \frac{g(t)}{t}\,dt. \tag{46}$$

Since $g(t)$ is known from Eq. (43), $j(t)$ can be evaluated according to (42), and therefore the right-hand sides of (44) and (45) are known.

5.2 Asymptotic solution of the aspiration length for a thick pipette

By introducing new unknown functions

$$y(x) = -\frac{\pi}{2b}g(bx), \qquad j_1(x) = \frac{\pi^2}{4b}j(bx), \tag{47}$$

we transform Eq. (43) as follows [11]:

$$y(x) + \frac{2}{\pi^2}\int_0^1 \frac{y(\sigma)}{x^2-\sigma^2}\left[\sigma \ln\Big(\frac{1-\lambda x}{1+\lambda x}\Big) - x\ln\Big(\frac{1-\lambda\sigma}{1+\lambda\sigma}\Big)\right]d\sigma = x. \tag{48}$$

While Eq. (48) holds for all values of $\lambda \in (0,1)$, approximate solutions can only readily be derived for small values of λ. Indeed, assuming that $\lambda \ll 1$ and applying a perturbation technique, we obtain its approximate solution in the form

$$\begin{aligned} y(x) = x &+ \lambda^3\frac{4x}{9\pi^2} + \lambda^5\frac{4x(5x^2+3)}{75\pi^2} + \lambda^6\frac{16x}{81\pi^4} \\ &+ \lambda^7\frac{4x}{735\pi^2}(35x^4+21x^2+15) + \lambda^8\frac{16x(5x^2+9)}{675\pi^4} + O(\lambda^9). \end{aligned} \tag{49}$$

Now, in view of (47) and (49), Eqs. (9) and (46) yield the aspiration length

$$L = \frac{4b\Delta P}{\pi M_3}\left\{1 + \frac{4\lambda^3}{9\pi^2} + \frac{56\lambda^5}{225\pi^2} + \frac{16\lambda^6}{81\pi^4} + \frac{116\lambda^7}{735\pi^2} + \frac{512\lambda^8}{2025\pi^4} + \dots\right\}. \tag{50}$$

Further, in view of (47), formula (45) takes the form

$$p(b\rho) = -\frac{2\Delta P}{\pi\rho}\frac{d}{d\rho}\left(\int\limits_0^1 \frac{xy(x)\,dx}{\sqrt{\rho^2-x^2}} + \frac{2}{\pi}\int\limits_{1/\lambda}^{\infty}\frac{xj_1(x)\,dx}{\sqrt{x^2-\rho^2}}\right). \tag{51}$$

Integrating the contact pressure density over the contact area, we evaluate the contact force

$$F = 2\pi\int\limits_b^a p(r)r\,dr = 2\pi b^2\int\limits_1^{1/\lambda} p(b\rho)\rho\,d\rho,$$

which after the substitution of (51) is represented as

$$\frac{F}{\pi b^2\Delta P} = 1 - \frac{4}{\pi^2}\int\limits_0^1 y(x)\ln\left(\frac{1+\lambda x}{1-\lambda x}\right)dx. \tag{52}$$

Thus, the substitution of the asymptotic expansion (49) into Eq. (52) results in the following expansion:

$$\begin{aligned}\frac{F}{\pi b^2\Delta P} = 1 - \frac{4}{\pi^2}\Bigg\{&\frac{2\lambda}{3} + \frac{2\lambda^3}{15} + \frac{8\lambda^4}{27\pi^2} + \frac{2\lambda^5}{35} + \lambda^6\frac{184}{675\pi^2}\\ &+ \lambda^7\Big(\frac{32}{243\pi^4} + \frac{2}{63}\Big) + \lambda^8\frac{12496}{55125\pi^2} + \ldots\Bigg\}.\end{aligned} \tag{53}$$

Finally, in view of (19) and (50), the pipette wall function is given by

$$\Phi_P(\eta) = 2\left\{1 + \frac{4\lambda^3}{9\pi^2} + \frac{56\lambda^5}{225\pi^2} + \frac{16\lambda^6}{81\pi^4} + \frac{116\lambda^7}{735\pi^2} + \frac{512\lambda^8}{2025\pi^4} + \ldots\right\}, \tag{54}$$

where the radii ratio λ is related to the wall parameter η by formulas

$$\lambda = \frac{1}{1+\eta}, \qquad \eta = \frac{1-\lambda}{\lambda}.$$

Note that since $\eta = (1-\lambda)/\lambda$ and $\eta \in (0, +\infty)$, the asymptotic expansion (54), which is valid as $\lambda \to 0$, holds only for large values of η.

5.3 Solution in the case of a free-standing half-space specimen

It is easily seen from formula (53) that the equilibrium equation (12) is not satisfied, because the contact force F is not equal to the total aspiration load $\pi b^2\Delta P$. Now, using the solution of contact problem for a flat-ended punch (see Section 54.2), we readily obtain the following formula for the aspiration length, L_0, of a free-standing half-space specimen:

$$L_0 = L + \frac{(\pi b^2\Delta P - F)}{\pi M_3 \mathbf{c}}(1-\psi). \tag{55}$$

Here, L is the aspiration length for a fixed specimen given by (50), $\mathbf{c}$ is the harmonic capacity of flat-ended punch given by (37), $\psi(\lambda)$ is the normalized surface deflection at the center of annular punch (see Fig. 5) given by (28), while the contact force F is given by formula (53).

So, making use of the asymptotic expansions (28), (37), and (53), we can evaluate the pipette wall function

$$\Phi_P^0(\eta) = \frac{\pi M_3}{2b\Delta P}L_0$$

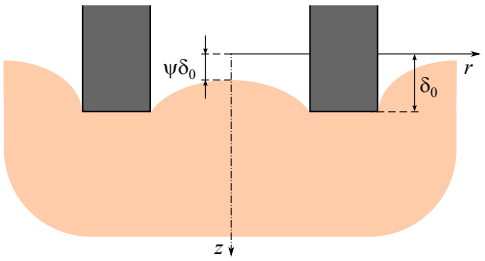

Figure 5: Center surface deflection for an annular flat-ended punch indented to a depth δ_0

as follows:

$$\Phi_P^0(\eta)=2+\frac{32\lambda^3}{9\pi^2}+\lambda^5\frac{896}{675\pi^2}+\lambda^6\frac{512}{81\pi^4} + \lambda^7\frac{23488}{33075\pi^2}+\lambda^8\frac{32768}{6075\pi^4}+O(\lambda^9). \tag{56}$$

Note that evidently $\Phi_P^0(\eta) > \Phi_P(\eta)$, while $\lim \Phi_P^0(\eta) = \lim \Phi_P(\eta) = 2$ as $\eta \to \infty$.

Finally, the aspiration displacement, according to (55), can be represented as

$$\delta_0 = -\frac{(\pi b^2 \Delta P - F)}{\pi M_3 \mathbf{c}}. \tag{57}$$

The application of the asymptotic expansions (37) and (53) in (57) allows us to derive the following approximation:

$$\delta_0=-\frac{4\lambda^2 b\Delta P}{3\pi M_3}\Big\{1+\frac{\lambda^2}{5}+\frac{16\lambda^3}{9\pi^2}+\frac{3\lambda^4}{35}+\frac{272\lambda^5}{225\pi^2} + \lambda^6\Big(\frac{256}{81\pi^4}+\frac{1}{21}\Big)+\lambda^7\frac{47024}{55125}+\ldots\Big\}. \tag{58}$$

Note that from (58) it is readily seen that $\delta_0 < 0$, meaning that the rigid displacement of the elastic specimen is directed towards the pipette.

6 Solution of the pipette aspiration problem for a narrow pipette

6.1 Aspirated length and aspiration approach

On the basis of the analysis performed in Section 3 (see Eqs. (15) and (16))), in the case of a free-standing half-space specimen, the aspirated length can be represented as

$$L_0 = -u_z^0(0) - \delta_0 + \frac{2}{M_3}\int\limits_b^a p_{-1}(\rho)\big(u_z^0(\rho)+\delta_0\big)\rho\, d\rho, \tag{59}$$

where, according to the generalized Mossakovskii's reciprocal theorem [37] (see also [38]), the contact pressure density $p_{-1}(r)$ satisfies the integral equation

$$\frac{1}{\pi M_3}\int\limits_0^{2\pi} d\phi \int\limits_b^a \frac{p_{-1}(\rho)\rho\, d\rho}{\sqrt{r^2+\rho^2-2r\rho\cos\phi}} = \frac{1}{r}, \quad r \in (b,a). \tag{60}$$

Thus, taking into account the relation

$$\frac{2}{M_3}\int\limits_b^a p_{-1}(\rho)\rho\, d\rho = \psi,$$

where ψ is the center surface deflection factor (see Eq. (39)), we reduce formula (59) to the following one:

$$L_0 = -u_z^0(0) + \frac{2}{M_3}\int\limits_b^a p_{-1}(\rho)u_z^0(\rho)\rho\,d\rho - (1-\psi)\delta_0. \tag{61}$$

Recall that the constant δ_0 is equal to zero for a fixed tested specimen, so that the corresponding aspirated length is given by

$$L = -u_z^0(0) + \frac{2}{M_3}\int\limits_b^a p_{-1}(\rho)u_z^0(\rho)\rho\,d\rho, \tag{62}$$

and thus, the two quantities L_0 and L are related as follows:

$$L_0 = L - (1-\psi)\delta_0. \tag{63}$$

Further, recall that in the case of a free standing specimen δ_0 should be determined from the equilibrium equation

$$\pi b^2\Delta P = 2\pi\int\limits_b^a p(\rho)\rho\,d\rho, \tag{64}$$

where $p(r)$ is the contact pressure density satisfying the integral equation (14) that is

$$\frac{1}{\pi M_3}\int\limits_0^{2\pi} d\phi\int\limits_b^a \frac{p(\rho)\rho\,d\rho}{\sqrt{r^2+\rho^2-2r\rho\cos\phi}} = -u_z^0(r) - \delta_0, r\in(b,a).$$

Now, first by application of Mossakovskii's reciprocal theorem [37], we transform Eq. (64) as

$$\pi b^2\Delta P = -2\pi\int\limits_b^a p_0(\rho)\big[u_z^0(\rho)+\delta_0\big]\rho\,d\rho. \tag{65}$$

Second, taking into account the relation

$$\mathbf{c} = \frac{2}{M_3}\int\limits_b^a p_0(\rho)\rho\,d\rho$$

for the harmonic capacity $\mathbf{c}$ of the annular punch, we resolve Eq. (65) for δ_0 as follows:

$$\delta_0 = -\frac{1}{M_3\mathbf{c}}\left(b^2\Delta P + 2\int\limits_b^a p_0(\rho)u_z^0(\rho)\rho\,d\rho\right). \tag{66}$$

Finally note that the integrals in (61) and (66) contain the function $u_z^0(r)$, which for $r\in(b,a)$ is given by the second formula (13).

6.2 Asymptotic solution for the aspirated length and aspiration approach

Making use of the variable change

$$r = R(1+\varepsilon\cos\alpha),\quad \alpha\in(0,\pi),\quad R=\frac{1}{2}(a+b),$$

we will have

$$u_z^0(r) = -\frac{4R\Delta P}{\pi M_3}(1+\varepsilon\cos\alpha)\Big\{\mathbf{E}\big(k(\varepsilon)\big) - \mathbf{K}\big(k(\varepsilon)\big)k'^2(\varepsilon)\Big\}. \tag{67}$$

Here we have introduced the notation

$$k(\varepsilon) = \frac{1-\varepsilon}{1+\varepsilon\cos\alpha}, \qquad k'(\varepsilon) = \sqrt{1-k^2(\varepsilon)}. \tag{68}$$

Observe that as $\varepsilon \to 0$, the modulus $k(\varepsilon)$ and the complementary modulus $k'(\varepsilon)$ behave as $k(\varepsilon) = 1 + O(\varepsilon)$ and $k'(\varepsilon) = O(\varepsilon^{1/2})$. Therefore, the following asymptotic series can be used [39]:

$$\mathbf{K}(k) = \Lambda' + \frac{k'^2}{4}(\Lambda' - 1) + \frac{9k'^4}{64}\Big(\Lambda' - \frac{7}{6}\Big) + \frac{25k'^6}{256}\Big(\Lambda' - \frac{37}{30}\Big) + \ldots, \tag{69}$$

$$\mathbf{E}(k) = 1 + \frac{k'^2}{2}\Big(\Lambda' - \frac{1}{2}\Big) + \frac{3k'^4}{16}\Big(\Lambda' - \frac{13}{12}\Big) + \frac{15k'^6}{128}\Big(\Lambda' - \frac{6}{5}\Big) + \ldots, \tag{70}$$

where

$$\Lambda' = \ln\frac{4}{k'}. \tag{71}$$

In view of (68) and (71), we readily get

$$\begin{aligned}\Lambda' = {} & \frac{\Lambda}{2} - \frac{\ln 2}{2} - \frac{1}{2}\ln(1+\cos\alpha) \\ & + \frac{\varepsilon}{4}(1+3\cos\alpha) + \frac{\varepsilon^2}{16}(1-2\cos\alpha-7\cos^2\alpha) \\ & + \frac{\varepsilon^3}{48}\big(1-3\cos\alpha+3\cos^2\alpha+15\cos^3\alpha\big) + \ldots,\end{aligned} \tag{72}$$

where $\Lambda = \ln(16/\varepsilon)$.

Let us introduce the notation

$$\mathcal{U}_z^0(\varepsilon,\alpha) = -\frac{\pi M_3}{4R\Delta P}u_z^0(r), \tag{73}$$

$$\mathcal{V}_0(\varepsilon,\alpha) = \frac{\varepsilon R}{\pi M_3}p_0(r)(1+\varepsilon\cos\alpha)\sin\alpha, \tag{74}$$

$$\mathcal{V}_{-1}(\varepsilon,\alpha) = Rv_{-1}(\varepsilon,\alpha), \tag{75}$$

where $u_z^0(r)$ is given by (67), and, in light of (30), the function $v_{-1}(\varepsilon,\alpha)$ determines the solution $p_{-1}(r)$ of Eq. (60).

By applying the asymptotic method of Grinberg and Kuritsyn [33], we find

$$\begin{aligned}\mathcal{V}_{-1}(\varepsilon,\alpha) = {} & \frac{1}{2\pi\Lambda} - \frac{\varepsilon}{4\pi}\cos\alpha \\ & + \frac{\varepsilon^2}{64\pi}\left[\left(10-\frac{3}{\Lambda}\right)\cos 2\alpha - 4 + \frac{6}{\Lambda} + \frac{8}{\Lambda^2}\right] \\ & - \frac{\varepsilon^3}{256\pi}\left\{\left(21-\frac{6}{\Lambda}\right)\cos 3\alpha + \left(17-4\Lambda+\frac{6}{\Lambda}\right)\cos\alpha\right\} + \ldots,\end{aligned} \tag{76}$$

while according to the asymptotic solution (32), we get

$$\begin{aligned}\mathcal{V}_0(\varepsilon,\alpha) = {} & \frac{1}{2\pi\Lambda} + \frac{\varepsilon}{4\pi}\cos\alpha \\ & + \frac{\varepsilon^2}{32\pi}\left[2 - \frac{5}{\Lambda} + \frac{4}{\Lambda^2} + \left(1-\frac{3}{2\Lambda}\right)\cos 2\alpha\right] \\ & + \frac{\varepsilon^3}{256\pi}\left\{\left(9-\frac{6}{\Lambda}-4\Lambda\right)\cos\alpha - \left(3-\frac{6}{\Lambda}\right)\cos 3\alpha\right\} + \ldots.\end{aligned}$$

Further, in light of (38), we put

$$\mathbf{c} = \pi R \mathcal{C}(\varepsilon), \tag{77}$$

where

$$\mathcal{C}(\varepsilon) = \frac{1}{\Lambda} + \frac{\varepsilon^2}{16}\left(2 - \frac{5}{\Lambda} + \frac{4}{\Lambda^2}\right) + \dots . \tag{78}$$

Thus, in view of (66), (73), and (74), the aspiration displacement can be represented as

$$\delta_0 = -\frac{R\Delta P}{\pi M_3 \mathcal{C}(\varepsilon)}\left((1-\varepsilon)^2 + 8\int_0^\pi \mathcal{U}_z^0(\varepsilon,\alpha)\mathcal{V}_0(\varepsilon,\alpha)\,d\alpha\right), \tag{79}$$

and the application of the asymptotic expansions (69)–(72), (76), and (78) allows us to derive from formula (79) the following approximation:

$$\delta_0 = -\frac{R\Delta P}{\pi M_3}\left\{\Lambda - 4 + \frac{\varepsilon^2}{16}\left(6\Lambda^2 - 11\Lambda + 8\right) + \dots\right\}. \tag{80}$$

Note that from (80) it is readily seen that $\delta_0 < 0$, since Λ is large for small ε. Fig. 6 illustrates the variation of δ_0 in the whole range of the pipette wall radii ratio λ; the difference between the asymptotic approximations (58) and (80) at the middle value $\lambda = 0.65$ is less than 0.15 %.

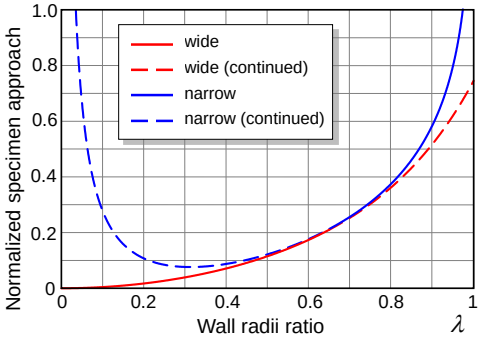

Figure 6: The normalized aspiration approach of the tested specimen $\delta_0 M_3/(b\Delta P)$. The red and blue lines are drawn according to the asymptotic approximations (58) and (80), respectively

6.3 Pipette wall functions for a narrow pipette

Using the above introduced notation (73)–(75), (77) and formulas (62) and (63), the pipette wall function in the case of a fixed specimen, $\Phi_P(\eta)$, and the pipette wall function in the case of a free-standing specimen, $\Phi_P^0(\eta)$, can be represented as follows:

$$\Phi_P(\eta) = \pi - \frac{4\pi}{1-\varepsilon}\int_0^\pi \mathcal{U}_z^0(\varepsilon,\alpha)\mathcal{V}_{-1}(\varepsilon,\alpha)\,d\alpha, \tag{81}$$

$$\Phi_P^0(\eta) = \Phi_P(\eta) + \frac{1-\psi}{2(1-\varepsilon)\mathcal{C}(\varepsilon)}\left((1-\varepsilon)^2 + 8\int_0^\pi \mathcal{U}_z^0(\varepsilon,\alpha)\mathcal{V}_0(\varepsilon,\alpha)\,d\alpha\right). \tag{82}$$

Here, η is the wall parameter, which is related to the wall thickness parameter ε by the formulas

$$\eta = \frac{2\varepsilon}{1-\varepsilon}, \qquad \varepsilon = \frac{\eta}{2+\eta}.$$

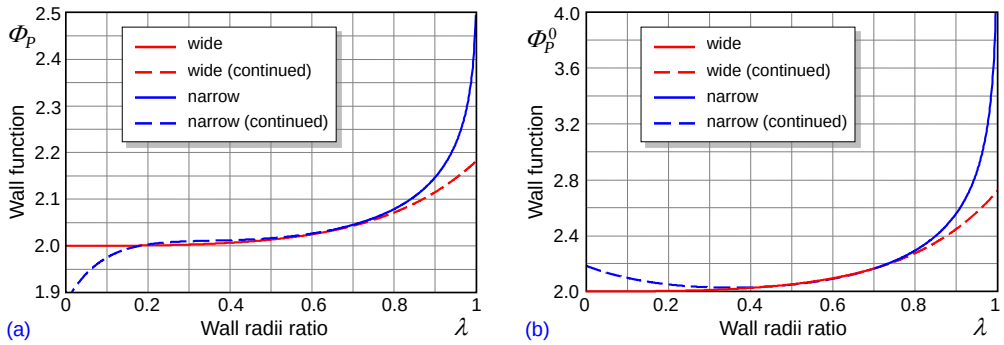

Figure 7: Asymptotic approximations for the pipette aspiration wall functions: (a) The red and blue lines are drawn according to the asymptotic approximations (54), (56) and (83), (84), respectively; (b) The blue lines are drawn according to the asymptotic approximations (83) and (84), respectively

Thus, making use of the asymptotic expansions (69)–(72), we obtain from Eqs. (81) and (82) the following approximations for the narrow pipette wall functions:

$$\Phi_P(\eta)=\pi-\frac{2\pi}{\Lambda}+\frac{\varepsilon\pi}{\Lambda}(\Lambda-2) - \frac{\varepsilon^2(1+\varepsilon)\pi}{4\Lambda^2}\big(\Lambda^3-6\Lambda^2+8\Lambda+2\big)+\ldots, \tag{83}$$

$$\Phi_P^0(\eta)=\frac{\Lambda}{2}+\frac{\pi}{2}-2+\frac{\varepsilon}{2}(\Lambda+\pi-4) + \frac{\varepsilon^2(1+\varepsilon)}{32\Lambda}\big[6\Lambda^3-(16\pi-5)\Lambda^2+56(\pi-1)\Lambda-32\pi\big]+\ldots. \tag{84}$$

Note also that since $\eta=2\varepsilon/(1-\varepsilon)$, the asymptotic expansions (83) and (84), which are valid as $\varepsilon\to 0$, hold only for small values of η.

Fig. 7 shows that the obtained asymptotic approximations allow one to evaluate the wall functions in the whole range of the pipette wall parameter λ; the difference between the predictions of the asymptotic approximations (54), (83) for $\Phi_P(\eta)$ and (56), (84) for $\Phi_P^0(\eta)$ in vicinities of the middle values $\lambda=0.65$ and $\lambda=0.70$ is less than 0.12 % and 0.14 %, respectively.

7 Discussion and conclusion

The objective of this study was to develop analytical tools to evaluate the local indentation stiffness of a soft tissue by means of pipette aspiration technique. The tissue was assumed to be transversely isotropic, macroscopically homogeneous, and linearly elastic, whereas the specimen surface was taken to be frictionless and flat near the tested point. In this regard, we developed asymptotic approximations in the half-space model framework, which was originally introduced by Theret et al. [11] and represents the deformation of a tested specimen by the deformation response of an elastic half-space. So that the specimen geometry and its characteristic size do not enter the resulting relation (3) for the aspirated length. A unique aspect of this study was the application of the generalized Mossakovskii's reciprocal theorem for evaluating the central surface deflection in the contact problem for an annular indenter.

Our analysis shows that it is of paramount importance to specify the boundary conditions of clamping for the tested specimen. In the framework of the half-space model they are accounted through the asymptotic conditions at infinity (see (11) and (12)). In particular, the following two configurations were considered: (a) Half-space specimen is fixed at infinity (configuration implicitly assumed in the punch model [11]); (b) Free-standing half-space specimen (configuration explicitly assumed in the FEM model [7]).

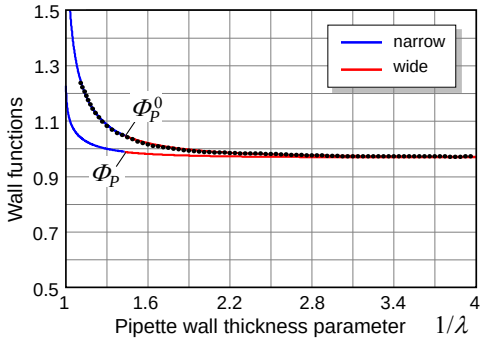

Figure 8: The scaled (after [7]) pipette aspiration wall functions in the isotropic case: $[2(1-\nu^2)/\pi]\Phi_P(\eta)$ due to the punch model for a fixed specimen, and $[2(1-\nu^2)/\pi]\Phi_P^0(\eta)$ due to the punch model for a free-standing specimen. The dotted line represents numerical results from [7] obtained for $\nu = 0.49$. (Note that $1/\lambda = 1+\eta$.)

Fig. 8 presents a direct comparison of the obtained asymptotic solutions with the results of FEM numerical simulations carried out by Aoki et al. [7] in the isotropic case for a nearly incompressible material, when $\nu = 0.49$. Note that a different normalization for the pipette wall function was adopted in [7]. Since the free-standing specimen configuration was used in [7], the numerical results (dotted line) fall onto the curve corresponding to $\Phi_P^0(\eta)$.

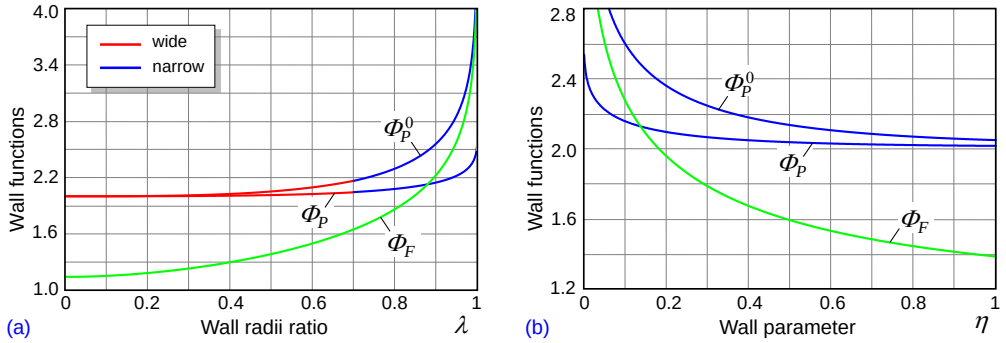

Figure 9: The pipette aspiration wall functions: $\Phi_F(\eta)$ due to the force model, $\Phi_P(\eta)$ due to the punch model for a fixed specimen, and $\Phi_P^0(\eta)$ due to the punch model for a free-standing specimen: (a) The red and blue lines are drawn according to the asymptotic approximations (54), (56) and (83), (84), respectively; (b) The blue lines are drawn according to the asymptotic approximations (83) and (84), respectively. In the both cases, the pipette aspiration wall function $\Phi_F(\eta)$ of the force model [11] was evaluated by means of formula (2)

To out knowledge, this study is the first report with explanations of the marked differences between predictions of the punch model $\Phi_P(\eta)$ and the force model $\Phi_F(\eta)$, both of which were introduced by Theret et al. [11]. Our fundings (see Fig. 9) imply that, from one side, the pipette wall function $\Phi_F(\eta)$ of the force model approaches the pipette wall function $\Phi_P^0(\eta)$ of a free-standing specimen as $\eta \to 0$, that is in the narrow pipette limit. From the other side, as is expected, the wall function $\Phi_P^0(\eta)$ goes close to the pipette wall function $\Phi_P(\eta)$ of the punch model [11] when $\eta \to +\infty$. Our findings indicate that the difference between $\Phi_P(\eta)$ and $\Phi_P^0(\eta)$ may be significant, especially in the case of a narrow pipette, when the wall parameter η is small.

Acknowledgement: The authors acknowledge support from EU project HORIZON2020 RISE Marie Sklodowska Curie grant MATRIXASSAY No 644175.

References

[1] Hochmuth RM. 2000 Micropipette aspiration of living cells. *J. Biomech.* **33**, 15–22.

[2] Haider MA, Guilak F. 2002 An axisymmetric boundary integral model for assessing elastic cell properties in the micropipette aspiration contact problem. *ASME J. Biomech. Eng.* **122**, 236–244.

[3] Lee LM, Liu AP. 2014 The application of micropipette aspiration in molecular mechanics of single cells. *J. Nanotechnol. Eng. Med.* **5**, 040902 (6 pp.).

[4] Lee LM, Liu AP. 2015 A microfluidic pipette array for mechanophenotyping of cancer cells and mechanical gating of mechanosensitive channels. *Lab Chip.* **15**, 264–273.

[5] Diridollou S, Patat F, Gens F, Vaillant L, Black D, Lagarde JM, Gall Y, Berson M. 2000 In vivo model of the mechanical properties of the human skin under suction. *Skin Res. Techn.* **6**, 214–221.

[6] Hollenstein M, Bajka M, Röhrnbauer B, Badir S, Mazza E. 2012 Measuring the in vivo behavior of soft tissue and organs using the aspiration device. *Soft Tissue Biomechanical Modeling for Computer Assisted Surgery, Studies in Mechanobiology, Tissue Engineering and Biomaterials*, Vol. 11, pp. 201–228.

[7] Aoki T, Ohashi T, Matsumoto T, Sato M. 1997 The pipette aspiration applied to the local stiffness measurement of soft tissues. *Annals Biomed. Eng.* **25**, 581–587.

[8] Kauer M, Vuscovic V, Dual J. 2001 Tissue aspiration and inverse finite element characterisation of soft tissues. *Comput. Meth. Biomech. Biomed. Eng.* **4**, 291–305.

[9] Weiß S, Thomson, SL, Lerch R, Döllinger M, Sutor A. 2013 Pipette aspiration applied to the characterization of nonhomogeneous, transversely isotropic materials used for vocal fold modeling. *J. Mech. Behav. Biomed. Mater.* **17**, 137–151.

[10] Buffinton CM, Tong KJ, Blaho RA, Buffinton EM, Ebenstein DM. 2015 Comparison of mechanical testing methods for biomaterials: Pipette aspiration, nanoindentation, and macroscale testing. *J. Mech. Behav. Biomed. Mater.* **51**, 367–379.

[11] Theret DP, Levesque MJ, Sato M, Nerem RM, Wheeler LT. 1988 The application of a homogeneous half-space model in the analysis of endothelial cell micropipette measurements. *J. Biomech. Eng.* **110**, 190–199.

[12] Alexopoulos LG, Haider MA, Vail TP, Guilak F. 2003 Alterations in the mechanical properties of the human chondrocyte pericellular matrix with osteoarthritis. *J. Biomech. Eng.* **125**, 323–333.

[13] Sakamoto M, Kobayashi K. 2004 The axisymmetric contact problem of an elastic layer subjected to a tensile stress applied over a circular region. *Theor. Appl. Mech. Japan* **53**, 27–36.

[14] Boudou T, Ohayon J, Arntz Y, Finet G, Picart C, Tracqui P. 2006 An extended modeling of the micropipette aspiration experiment for the characterization of the Young's modulus and Poisson's ratio of adherent thin biological samples: Numerical and experimental studies. *J. Biomech.* **39**, 1677–1685.

[15] Sato M, Theret DP, Wheeler LT, Ohshima N, Nerem RM. 1990 Application of the micropipette technique to the measurement of cultured porcine aortic endothelial cell viscoelastic properties. *J. Biomech. Eng.* **112**, 263–268.

[16] Delafargue A, Ulm F-J. 2004 Explicit approximations of the indentation modulus of elastically orthotropic solids for conical indenters. *Int. J. Solids Struct.* **41**, 7351–7360.

[17] Yu HY. 2001 A concise treatment of indentation problems in transversely isotropic half-spaces. *Int. J. Solids Struct.* **38**, 2213–2232.

[18] Gubenko VS, Mossakovskii VI. 1960 Pressure of an axially symmetric circular die on an elastic half-space. *J. Appl. Math. Mech.* **24**, 477–486.

[19] Shibuya T, Koizumi T, Nakahara I. 1974 An elastic contact problem for a half-space indented by a flat annular rigid stamp. *Int. J. Eng. Sci.* **12**, 759–771.

[20] Barber JR. 1976 Indentation of the semi-infinite elastic solid by a concave rigid punch. *J. Elast.* **6**, 149–159.

[21] Dhawan GK. 1979 A transversely isotropic half-space indented by a flat annular rigid stamp. *Acta Mech.* **31**, 291–299.

[22] Gladwell GML, Gupta OP. 1979 On the approximate solution of elastic contact problems for a circular annulus. *J. Elast.* **9**, 335–348.

[23] Antipov YA. 1989 Analytic solution of mixed problems of mathematical physics with a change of boundary conditions over a ring. *Mech. Solids* **24**(3), 49–56.

[24] Kesari H, Lew AJ. 2011 Adhesive Frictionless Contact Between an Elastic Isotropic Half-Space and a Rigid Axi-Symmetric Punch. *J. Elasticity* **106**, 203–224.

[25] Kesari H, Lew AJ. 2011 Effective macroscopic adhesive contact behavior induced by small surface roughness. *J. Mech. Phys. Solids* **59**, 2488–2510.

[26] Argatov I, Li Q, Pohrt R, Popov VL. 2016 Johnson–Kendall–Roberts adhesive contact for a toroidal indenter. *Proc. Royal Soc. A* 20160218. http://dx.doi.org/10.1098/rspa.2016.0218.

[27] Argatov II, Sabina FJ. 2015 Small-scale indentation of a hemispherical inhomogeneity in an elastic half-space. *Eur. J. Mech. A/Solids* **53**, 151–162.

[28] Love AEH. 1929 The stress produced in a semi-infinite solid by pressure on part of the boundary. *Philos. Trans. Roy. Soc. London. Ser. A* **228**, 377–420.

[29] Johnson KL. 1985 *Contact Mechanics.* Cambridge, UK: Cambridge University Press.

[30] Hanson MT, Puja IW. 1996 Love's circular patch problem revisited closed form solutions for transverse isotropy and shear loading. *Q. Appl. Math.* **54**, 359–384.

[31] Collins WD. 1963 On the solution of some axisymmetric boundary value problems by means of integral equations. *Proc. Edinb. Math. Soc. III* **13**, 235–246.

[32] Jain DL, Kanwal RP. 1972 Three-part boundary value problems in potential and generalised axially symmetric potential theories. *J. Analyse Math.* **25**, 107–158.

[33] Grinberg GA, Kuritsyn VN. 1962 Diffraction of a plane electromagnetic wave by an ideally conducting plane ring and the electrostatic problem for such a ring. *Tech. Phys.* **6** 743–749.

[34] Pólya G, Szegö G. 1951 *Isoperimetric Inequalities in Mathematical Physics.* Princeton, NJ: Princeton University Press.

[35] Galin LA. 2008 *Contact Problems: The Legacy of L.A. Galin.* Ed. G.M.L. Gladwell, Dordrecht: Springer.

[36] Argatov I. 2010 Frictionless and adhesive nanoindentation: Asymptotic modeling of size effects. *Mech. Mater.* **42**, 807–815.

[37] Mossakovskii VI. 1951 Estimating displacements in spatial contact problems [in Russian]. *J. Appl. Math. Mech. (PMM)* **15**, 635–636.

[38] Argatov II. 2001 The pressure of a punch in the form of an elliptic paraboloid on an elastic layer of finite thickness. *J. Appl. Math. Mech.* **65**, 495–508.

[39] Jahnke E, Emde F, Lösch F. 1977 *Special Functions: Formulae, Graphs, Tables* [Russian translation]. Moscow: Nauka.